Direction-dependent initial-state relaxation in oxygen K x-ray emission

J. Valjakka, J. Utriainen, T. Åberg, and J.Tulkki

Laboratory of Physics, Helsinki University of Technology, SF-02150 Espoo, Finland

(Received 27 March 1985)

High-resolution oxygen K x-ray spectra have been obtained from a number of ionic insulators. A distortion of the $1s^{-1}$-V^{-1} x-ray emission band due to the initial $1s$ hole is observed and related to the variation in the $1s^{-1}V^{-1}$-V^{-2} satellite structure as a function of the bonding character. A shake model which considers the influence of the crystal environment on the relaxation of the O^{2-} $2p$ orbitals is shown to account for the diminution of the satellite intensity with increasing covalency.

I. INTRODUCTION

X-ray valence-band (VB) spectra not only reflect the unperturbed band structure, but also the response of the valence electrons to the creation of the initial inner-shell vacancy.[1] For metals this many-body relaxation phenomenon has been extensively studied.[2] For semiconductors and insulators our knowledge of the influence of the initial-state relaxation effect is poor, although in many cases oscillator-strength distributions based on unperturbed Bloch states seem to agree with the shape of measured x-ray-band spectra, indicating no appreciable effect of the hole other than lifetime broadening.[3]

In this work we show that in insulators the influence of the initial-state relaxation on x-ray emission bands can be remarkable. The observed dramatic narrowing of the $1s^{-1}$-V^{-1} emission band in certain oxides is found to be linked with the appearance of an intense resolved $1s^{-1}V^{-1}$-V^{-2} satellite structure. This result indicates that the distortion of the band and the change of the satellite intensity have a common origin, related to the electronic structure in the crystal environment of the oxygen ion. By assuming that the redistribution of the valence electrons around the suddenly created K hole is direction dependent, the simultaneous variation in both the emission band and the satellite structure is qualitatively explained. Any other effects, such as the dependence of the band shape on the valence- to $1s$-state transition probability,[3,4] final-state hole-hole correlation,[5] and initial-state electron transfer from double- to separate single-hole states[6] are ruled out as the major cause for the structural dependence of the oxygen K x-ray emission.

II. EXPERIMENTAL

Our oxygen K-emission spectra were obtained using a grazing-incidence spectrometer, equipped with a gold-coated 6.0-m radius grating with 600 lines per mm. The powder specimens were rubbed on a water-cooled copper anode and excited by (4–6)-keV electrons forming a current of typically 25 mA. The pressure in the x-ray tube was 2×10^{-4} Pa. A spherical polystyrene-coated glass mirror was set at an 1.43° grazing angle between the focus of the x-ray tube and the entrance slit to suppress the high-energy radiation. The entrance- and receiving-

slit widths were 10 μm, resulting in an energy resolution of 0.35 eV at the oxide $K\alpha$ energy in second order. The detector was a proportional counter with an ~ 200 nm nitrocellulose window, filled with a 10% argon-methane mixture at normal pressure. The following oxide samples were studied: Li_2O, BeO, MgO, Al_2O_3, SiO_2, CaO, Sc_2O_3, TiO, TiO_2, SrO, and BaO. In each case a search for impurity lines was made and the crystalline structure was checked by x-ray diffraction whenever uncertain.

III. RESULTS

An examination of our data and earlier photographic recordings[7] indicates that all oxide K spectra recorded so far fall basically into three categories, depending on the form of the structure in the range from $+1$ to $+4$ eV *above* the main peak, $K\alpha$. As typical spectra in Fig. 1 indicate, there are at least two peaks, α_3 and α_4, in category (a). In category (b) there is only one peak, α_4, and in (c) there are no peaks at all. Instead, there is in all spectra a broad structure above $+4$ eV, appearing with a target-independent relative intensity of the order of 7% with respect to the K-emission-band intensity. As shown in Fig. 1, the main peak has a pronounced low-energy shoulder below -1 eV in (b)- and (c)-type spectra but not in (a)-type spectra.

In the following we shall exclude the transition-metal oxides where the emission from the d bands may also contribute to the high-energy structure. However, as is exemplified by our Sc_2O_3 spectrum in Fig. 1, many transition-metal and rare-earth oxide spectra[7] seem to fall into category (b). In Table I, which lists our results, N is the number of positive ions surrounding the oxygen ion and ΔE is the separation between $\alpha_{3(4)}$ and α. The integrated intensity I of the satellite structure between $+1$ and $+4$ eV is given relative to the total K-emission-band intensity. Our values of the basewidth W of the K band (x ray) are compared with results of x-ray photoelectron spectroscopy (XPS) measurements[8–10] and of calculations of the density of states (DOS).[11–15] Estimated errors are ± 0.1 eV for ΔE, $\pm 3\%$ for I, and ± 0.5 eV for W (x ray).

The most striking result emerging from Table I and Fig. 1 is that the intense (a)-type satellite structure is accompanied by a very narrow and nearly symmetric K-emission band. As is indirectly indicated by the narrow
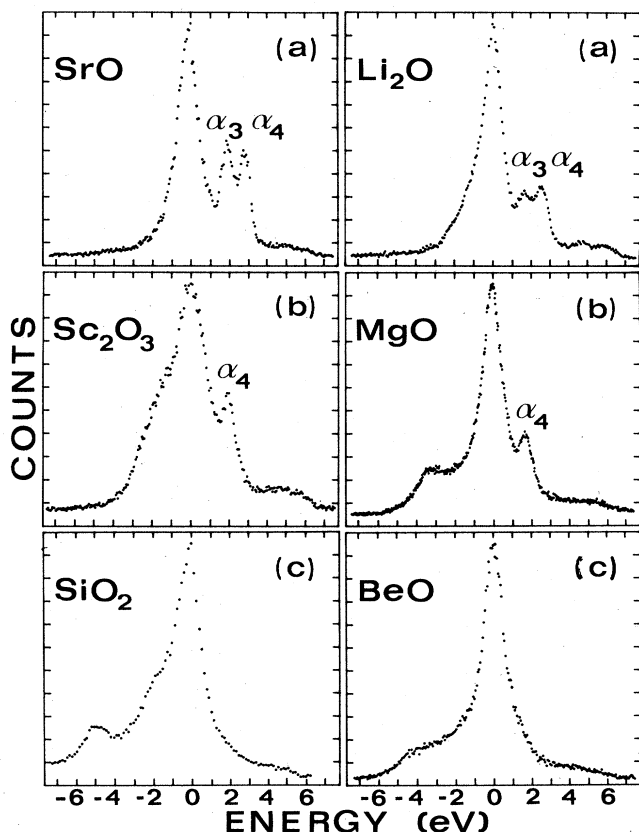
FIG. 1. Oxygen K-emission spectra in the energy range 518–532 eV. The energies are given relative to the maximum of the main peak $K\alpha$. The spectra are classified in the text according to whether there are (a) two peaks, α_3 and α_4, (b) one peak, α_4, and (c) no peaks at the high-energy side of $K\alpha$.

x-ray widths as compared with the XPS and DOS widths, this form of the K band does not reflect the ground-state valence-band structure at all. The reason for this could be twofold. Either the emission band is governed by a strong distorting effect caused by the wave-vector dependence of the VB-to-1s transition probability, or it is due to the in-

fluence of the 1s hole on the valence electrons. As shown in the next section, transition-probability arguments do not lead to a satisfactory explanation of the unusual band shape.

IV. COMPARISON WITH DOS AND XPS

The traditional theory[3,4] of x-ray emission from valence bands attributes the intensity distribution of $1s^{-1}$-V^{-1} transitions to the one-electron intensity distribution

$$I(\omega)=2\pi\sum_{\mathbf{k}}|\langle\mathbf{k}|T|1s\rangle|^2\delta(\epsilon_{\mathbf{k}}-\epsilon_{1s}-\omega)\ ,\qquad(1)$$

where the summation over the wave vector $\mathbf{k}$ extends over all ground-state Bloch states $|\mathbf{k}\rangle$ of the valence band. The transition matrix element $\langle\mathbf{k}|T|1s\rangle$ selects the p symmetry of each state $|\mathbf{k}\rangle$ with respect to the oxygen site. Thus in the tight-binding (TB) approach, $I(\omega)\propto N_p(\omega)$, where the partial p density of states $N_p(\omega)$ (p-DOS) is defined by

$$N_p(\omega)=\sum_{\mathbf{k},v}|C_v(\mathbf{k})|^2\delta(\epsilon_{\mathbf{k}}-\epsilon_{1s}-\omega)\ .\qquad(2)$$

In Eq. (2), $C_v(\mathbf{k})$ is the expansion coefficient of the $2p_v$ ($v=x,y,z$) oxygen orbital in the Bloch state $|\mathbf{k}\rangle$. The choice of the directions x, y, and z is dictated for each crystal by the symmetry and nearest-neighbor structure of the oxygen site with the 1s hole.

Since accurate evaluations of $N_p(\omega)$ do not exist for all the materials listed in Table I, one has to examine the results of calculations[11–15] of the full DOS. In spite of the structural differences,[16] their valence bands share a number of common points with regard to the p symmetry.[11–15] Notably, the DOS is divided into two regions by a dip at 0.4 to 0.6 times the basewidth W. Above this there are mostly bands with oxygen $2p$ nonbonding character. Below the dip the bands are formed from oxygen $2p$ bonding orbitals with some mixing of the outermost s and p orbitals of the neutral cation.

Even a limited basis set consisting of oxygen $2p_v$ ($v=x,y,z$) orbitals leads to a satisfactory description of the valence band of the rocksalt-type crystals MgO, CaO,

TABLE I. Correlation between the satellite structure and the width of the oxygen K x-ray emission band.

Target	N	Type	ΔE (eV) α_3	α_4	I (%)	X ray	W (eV) XPS[d]	DOS[e]
BaO	6	a	1.9	2.8	32	3.0	9	4.1
SrO	6	a	1.9	2.8	36	2.6	10	4.7
CaO	6	a	1.7	2.8	33	2.7	8	8.4
Li$_2$O	8	a	1.6	2.6	21	4.2		5.8
MgO	6	b		1.7	9	6.5	6.5	8.5
Al$_2$O$_3$	4	c				9.5	11.6	6.5
BeO	4	c				7.5		6
SiO$_2$	2	c				11.5	12	13

[a] Category (a) from text.
[b] Category (b) from text.
[c] Category (c) from text.
[d] Reference 8, except for W in SiO$_2$ and for W in CaO and BaO, which are taken from the figures of Refs. 9 and 10, respectively.
[e] Reference 11 (BaO, SrO), Ref. 12 (MgO, CaO), Ref. 13 (Al$_2$O$_3$), Ref. 14 (BeO), and Ref. 15 (SiO$_2$). The empirical tight-binding method of Ref. 5 was used to estimate the Li$_2$O width by assuming a fcc O^{2-} sublattice without Li$^+$ ions.

SrO, and BaO, provided the p-bonding matrix element is adjusted by an accurate band calculation for some of the crystals.[11] Here x and y point in the [110] directions, whereas z points toward the cations in the [100] directions. Thus the combined evidence of Ref. 11 and more elaborate band calculations[12-15] show that any reasonable choice of the Bloch state $|k\rangle$ would result in p symmetry throughout the band. The variation of the coefficients $C_\nu(k)$ in Eq. (2) as a function of ϵ_k can only be such that even though the transitions from the oxygen $2p$ bonding orbitals would get less weight in comparison with those from the nonbonding orbitals, they would not entirely vanish. This is precisely the behavior found in the (b)- and (c)-type K bands, as is exemplified by the thorough theoretical analyses of this band in SiO_2.[15] Thus, although an approach based on Eq. (1) would account for the shape of these bands, it certainly would fail to account for the unusual shoulderless form of (a)-type bands.

Equation (1) should apply to XPS provided $\langle k\,|\,T\,|\,1s\rangle$ is replaced by $\langle c\,|\,T\,|\,k\rangle$, where c is the continuum wave function of the photoelectron. Since the latter matrix element is a slowly varying function of k, XPS spectra should reflect the shape of the full DOS better than x-ray spectra. A comparison of data in Refs. 8–10 with calculations[11,13,15] roughly confirms the universal shape of DOS described above, although the XPS spectra predict substantially wider valence bands for Al_2O_3, SrO, and BaO. As shown in Table I, W(x ray) is only one-third of W(XPS) in CaO, SrO, and BaO, supporting the conclusion that the unusual (a)-type band shapes are not merely due to variations in the matrix element $\langle k\,|\,T\,|\,1s\rangle$.

V. INITIAL-STATE RELAXATION AND THE HIGH-ENERGY SATELLITE STRUCTURE

A. Band model

Equation (1) does not account for the initial-state relaxation of the valence electrons since it employs ground-state Bloch functions for the $1s$-hole state. Within the one-electron framework this assumption leads to zero probability for multiple excitation. In particular, this approach does not account for the formation of $1s^{-1}V^{-1}$ double-hole states, which, as we shall show, are responsible for the satellite structure between $+1$ and $+4$ eV. Consequently, a consistent one-electron theory of the *entire* K x-ray emission structure requires the introduction of $1s$-hole-distorted Bloch states $|k^*\rangle$. Instead of Eq. (1), we have, in lowest order of the overlap matrix elements[2] $\langle k\,|\,k^*\rangle$,

$$I^*(\omega)=2\pi\sum_k\left|\sum_{k'}\langle 1s\,|\,T\,|\,k'\rangle\langle k'\,|\,k^*\rangle\right|^2\delta(\epsilon_k-\epsilon_{1s}^*-\omega)\;,$$

(3)

where the summation over k' should be carried over all excited conduction-band states as well. The $1s$ ionization energy $-\epsilon_{1s}^*$ includes the $1s$ relaxation-energy shift.

Although an accurate evaluation of the intensity expression (3) is out of range for any of the oxides in Table

I, a few qualitative comments can be made. It follows from Eq. (3) that $I^*(\omega)\propto N_p^*(\omega)$, where the modified partial p-DOS is given by

$$N_p^*(\omega)=\sum_{k,\nu}\left|\sum_{k'}C_\nu(k')\langle k'\,|\,k^*\rangle\right|^2\delta(\epsilon_k-\epsilon_{1s}^*-\omega)\;.$$

(4)

There are two limiting cases with regard to the influence of the overlap elements $\langle k\,|\,k^*\rangle$. Either $\langle k\,|\,k^*\rangle\simeq\delta_{k,k^*}$ so that Eq. (2) is a good approximation but with ϵ_{1s} replaced by ϵ_{1s}^*, or the $1s$ hole distorts the valence-band states to the extent that they become localized and nonbonding. In the latter case, Eq. (4) reduces approximately to

$$N_p^*(\omega)\simeq{\sum_{k,\nu}}'\,|\,C_\nu(k)\,|^2\,\langle 2p_\nu\,|\,2p_\nu^*\rangle^2\delta(\epsilon_k-\epsilon_{1s}^*-\omega)\;,$$

(5)

where the prime indicates a summation over the nonbonding states only. Thus it follows from Eq. (4) that the shape of the oxygen K x-ray emission band may not necessarily reflect the entire p-DOS but only the nonbonding part of it, in accordance with the suggestion concerning (a)-type emission bands in Sec. IV. The position of the band is predicted to be at $\omega=\epsilon_k-\epsilon_{1s}^*$ in both cases. Furthermore, in the strong-distortion limit (5), the probability that the valence electrons keep their quantum numbers is given by the factor $\langle 2p_\nu\,|\,2p_\nu^*\rangle^2$, where $2p_\nu$ is the x, y, or z oxygen $2p$-orbital result, is in accord with the "shake" theory of x-ray satellites,[17] which would attribute the probability $1-\langle 2p_\nu\,|\,2p_\nu^*\rangle^2$ to the excitation of a $2p_\nu$ electron during the $1s$ ionization process.

The multiple-excitation process leads to formation of $1s^{-1}V^{-1}$ double-hole states which decay into V^{-2} states by radiative transitions. They may show up as separate satellite lines or they may blend with the main emission band, depending on the degree of localization of the distorted Bloch states $|k^*\rangle$. As shown in the next section, the strong-distortion limit (5) leads necessarily to separate satellites on the high-energy side of the $K\alpha$ line. Hence it seems clear that an interpretation of the oxygen K x-ray emission spectra is not possible without considering the initial-state relaxation.

B. Ion model

Although the oxides considered here have wide valence-band widths, they also have rather large optical band gaps (≥ 5 eV), typical for ionic crystals. Hence we shall in the following make a prediction of the entire K x-ray emission spectrum by assuming a pure ionic bond. This result will also indicate what the intensity distribution would be in the strong-distortion limit (5), since in the ionic model there are only nonbonding orbitals. A comparison is made with the results in Table I concerning the (a)-type spectra.

Since the O^{2-} ion does not exist as a free ion the ion model requires the construction of a neonlike oxygen pseudoion which simulates its charge distribution in the crystal environment.[18] This we have done by incorporating in the atomic Hartree-Fock procedure the Watson-sphere correction,[19] which accounts for the stabilization

of the O^{2-} ion in a cubic crystal environment. The parameters used in Watson's potential U ($U=Q/R_0$ for $R_0 \leq R$ and $U=Q/R$ for $R>R_0$) were $Q=+2$ and $R_0=2.76$ a.u., the latter being the standard crystal radius for O^{2-}. The response of the valence electrons to the O^{2-} $1s$ hole can then be calculated by assuming a fully localized hole and by assigning to each ion in the lattice a charge and polarizability. This leads, in accordance with the local-hole point-ion model of Mahan,[20,21] to a formula for the ionization energy of one or two electrons in both O^{2-} and the cation. The result is

$$I(n)=I'(n)\pm nE_M-E_P(n)-E_R(n) , \qquad (6)$$

where all quantities are defined as positive and where $I'(n)$ is any of the single- ($n=1$) or double- ($n=2$) ionization energies in the O^{2-} pseudoion or in the cation. In Eq. (6), E_M is the Madelung energy, with the plus sign referring to O^{2-} and the minus sign to the cation. The ionization energy $I'(n)$ includes the intraionic relaxation energy, whereas $E_P(n)$ describes the polarization of the surrounding ions by one or two holes, representing the extraionic relaxation. There is also a contribution from the change in the repulsion energy $E_R(n)$ due to the formation of the holes. According to Mahan,[20] $E_P(n)$ is split into the classical Mott-Littleton polarization energy $\Sigma_{ML}(n)$ and an additional contribution $\Sigma_2(n)$, proportional to the hole charge. Hence, in the linear approximation, $E_P(2)=4\Sigma_{ML}(1)+2\Sigma_2(1)$. Although the calculation of $E_P(n)$ and $E_R(n)$ should be consistent with the adopted pseudoion model of O^{2-}, one may use Mahan's results[21] for estimating the ionization energies in the fcc oxides of Table I.

In this section we need only one consequence of Eq. (6), namely that the K x-ray transition energies of O^{2-} are predicted for both $n=1$ and 2 by the differences $I'_{1s}(n)-I'_{2p}(n)$, which can be calculated by using the modified Hartree-Fock (HF) ΔE_{SCF} procedure (SCF denotes self-consistent field). For $n=1$ the result is 526.0 eV, in agreement with the position of the $K\alpha$ peak, which varies slightly between 525 and 526 eV depending on the target material.[22]

According to the ion model, the high-energy satellite structure of the O^{2-} $K\alpha$ line should resemble that of the $K\alpha$ line in isoelectronic Ne. In LS coupling the resulting $1s^{-1}2p^{-1}$-$2p^{-2}$ dipole-allowed transitions are ^3P-^3P (α_3), ^1P-^1D (α_4), and ^1P-^1S (α'), with their statistical intensity ratios given by 9:5:1 and with their Ne identification scheme[23] given in parentheses. The $1s^{-1}2s^{-1}$-$2s^{-1}2p^{-1}$ transitions can be neglected as weak in comparison with $1s^{-1}2p^{-1}$-$2p^{-2}$ transitions. The modified HF procedure gave $\Delta E_{\alpha_3}=+1.9$ eV and $\Delta E_{\alpha_4}=+2.4$ eV, in good agreement with the experimental values in Table I for (a)-type spectra. Even α' can be seen at $\Delta E\simeq+0.6$ eV as a small hump in the CaO, SrO, and BaO intensity curves.

It is also possible to use, in accordance with Eq. (5), the overlap matrix element $\langle 2p \mid 2p^* \rangle$ between the ground-state and $1s$-hole pseudoion $2p$ wave functions for a prediction of the total relative satellite intensity I.[17] If the transition-rate corrections are neglected, I is given by the total relative probability P_{2p} of exciting any one of the six $2p$ valence electrons in association with the $1s$ ionization.

According to the shake model,[17]

$$P_{2p}=6(1-\langle 2p \mid 2p^* \rangle^2)/\langle 2p \mid 2p^* \rangle^2 , \qquad (7)$$

which yields $I=35.3\%$, in good agreement with the experimental values for the (a)-type targets, except for Li_2O, as shown in Table I.

In our experiment the spectra are excited by energetic electrons, which ensures the validity of the shake model. Due to the spread of the incoming beam in the target, there is no directional preference for populating the magnetic substates of $1s^{-1}2p^{-1}$ $^{1,3}P$ unequally.[24] Nevertheless, as indicated by the Li_2O and SrO spectra in Fig. 1, the ratio of α_3 and α_4 is closer to 1 than the statistical ratio 9:5 for all (a)-type spectra. As will be shown in Sec. VI B, this effect can be attributed to mixing between the excited initial $(1s^{-1}2p^{-1}$ $^{1,3}P)\epsilon p$ ^2S states, where ϵp denotes a final shake-up or shake-off electron. Another effect not predicted by the ion model is the width of the $K\alpha$ line, which is about 4 times broader for the (a) case than is expected from the approximate $1s$ lifetime width 0.2 eV. According to Eq. (5), this may be attributed to the modified p-DOS of primarily nonbonding $2p^*$ orbitals.

VI. DIRECTION-DEPENDENT RELAXATION MODEL

According to Fig. 1 and Table I, the Li_2O and MgO spectra show a high-energy satellite structure that is weaker in intensity than predicted by the ion model. Furthermore, MgO has only one satellite peak in association with a pronounced low-energy shoulder of the $K\alpha$ peak. These features are discussed in the following two subsections.

A. Total satellite intensity

The diminution of the satellite intensity can be understood by a simple geometrical model of the initial-state relaxation. Both in Li_2O and MgO the oxygen ions form a fcc sublattice. However, in Li_2O each oxygen is surrounded by a cube of eight Li^+ ions, whereas in MgO there are only six adjacent Mg^{2+} ions in the [100] directions. According to Sec. III the valence-band structure of MgO can be described by choosing a bonding unit[25] that consists of the O^{2-} $2p_v$ ($v=x,y,z$) orthogonal orbitals. In this unit x and y point toward the oxygen ions in the [110] directions and z toward the Mg^{2+} ion in the [100] direction. If a similar unit is chosen for the antifluorite Li_2O, the crystal symmetry requires that x and y point toward the Li^+ ions at the corners of the surrounding cube and that z point toward O^{2-} in the adjacent cube. Hence the roles of the $2p_z$ and the $2p_{x,y}$ orbitals are interchanged in going from MgO to Li_2O.

In both crystals there is a strong bond formation between the oxygen ions. This is illustrated by the fact that in MgO the O^{2-}-O^{2-} wave-function overlap in comparison with the cation-O^{2-} overlap is 4 times larger than it is in CaO.[26] Hence one may assume that the relaxation leads to the formation of localized nonbonding $2p_v^*$ states only in the positive-ion directions. In Li_2O these would be $2p_x^*$ and $2p_y^*$, and in MgO, $2p_z^*$. Consequently, according

to Eq. (7) and our modified HF calculations, $I = \frac{2}{3} P_{2p} \simeq 24\%$ for Li_2O and $I = \frac{1}{3} P_{2p} \simeq 12\%$ for MgO, in good agreement with the corresponding experimental values in Table I.

According to Sec. V A the strength of the separate satellite structures should monitor the shape of the K-emission band. The distortion due to the $1s$ hole should gradually disappear, i.e., the bandlike emission should be recovered when the satellite intensity becomes stepwise smaller. According to Fig. 1 the emission band of Li_2O is somewhat more asymmetric than that of SrO. In MgO the shape and width of the band resemble those of the p-DOS. This result is consistent with the analysis of Sec. IV, which showed that O^{2-}-O^{2-} bonding orbitals which remain delocalized in $1s$ ionization are primarily responsible for the low-energy part of the p-DOS. Once the average number of positive ions surrounding the oxygen ion is less or equal to 4, as for the noncubic target compounds in Table I, no separate satellites are observed. Consequently, the bonding-orbital structure is preserved, showing itself as the low-energy shoulder of the $K\alpha$ line.

The absence of the separate satellite structure in (c)-type spectra does not imply that no $1s^{-1}V^{-1}$ states are formed. In fact, it follows from Sec. V B that the position of the $K\alpha$ peak for each target compound in Table I is consistent with a relaxation-energy shift $\epsilon_{1s}^{*} - \epsilon_{1s} \simeq 30$ eV. This, in turn, implies, according to the sum rule of Manne and Åberg,[27] that in (c)-type spectra the $1s^{-1}V^{-1}$-V^{-2} satellite transitions have merged into the K-emission band. This is illustrated by the fact that if one normalizes the $K\alpha$ peak height to 1, all targets have the same integrated intensity within $\pm 10\%$ in the -4 to $+4$ eV range, which also includes the separate satellite structure whenever it exists. The lower bound, -4 eV, corresponds approximately to the dip in the DOS between the bonding and antibonding parts. Furthermore, the p-DOS calculations for SiO_2 predict a $K\alpha$ peak which is too low,[15] indicating an underlying structure.

B. The α_3 to α_4 intensity ratio

In this section it is shown that the direction-dependent relaxation model can be extended to account for the anomalous $I(\alpha_3)/I(\alpha_4)$ ratio and, eventually, also for the one-peak satellite structure in MgO. Analogous to electron shake off in Ne,[28,29] it requires considerations of the final ϵp shake-up and shake-off states of the $2p$ valence electrons formed in the $1s$ ionization process.

Let us first consider the situation in a free neonlike ion. Due to the monopole selection rules the many-electron wave functions of the final $1s^{-1}2p^{-1}\epsilon p$ configurations must have the same symmetry and parity as the $1s^{-1}{}^{2}S$ states. Within the one-electron framework they can be classified either as $1s[2p^5\epsilon p\,^{1,3}S]^2 S$ or $[1s2p^{5\,1,3}P]\epsilon p\,^2S$ states, depending on the order of the angular-momentum coupling.[28] The former description is adequate if the ϵp state is bound and strongly coupled to the $2p^5$ shell. The latter choice prevails if the coupling between the open $1s$ and $2p^5$ shells is stronger than that between $2p^5$ and ϵp. In general, one expects a situation which is between these two extreme cases. The corresponding final shake-up or

shake-off states can then be described by a linear superposition $\phi_{\gamma} = C_{\gamma t} \, | \, t \, \rangle + C_{\gamma s} \, | \, s \, \rangle$ $(\gamma = 1,2)$ of the triplet state $| \, t \, \rangle = 1s[2p^5\epsilon p\,^3S]^2 S$ and the singlet state $| \, s \, \rangle = 1s[2p^5\epsilon p\,^1S]^2 S$. The coefficients $C_{\gamma t}$ and $C_{\gamma s}$ are obtained by diagonalizing the corresponding two-by-two Hamiltonian matrix $\mathbf{H}$. Subtracting the common energy part of $E_t = \langle t \, | \, H \, | \, t \, \rangle$ and $E_s = \langle s \, | \, H \, | \, s \, \rangle$,

$$\mathbf{H} = \frac{1}{3} \begin{bmatrix} G_c^1 + G^1 - \frac{1}{2}G^0 & (\sqrt{3}/2)(G_c^1 - G^1) \\ (\sqrt{3}/2)(G_c^1 - G^1) & \frac{35}{2}G^0 \end{bmatrix}, \quad (8)$$

where $G_c^1 = G^1(1s,2p)$, $G^1 = G^1(1s,\epsilon p)$, and $G^0 = G^0(2p,\epsilon p)$ in the usual notation of Slater exchange integrals.

If it is assumed that the electron in the ϵp state remains a spectator electron during the emission process, then there are only the $[1s2p^{5\,3}P]\epsilon p\,^2S - [2p^{4\,3}P]\epsilon p\,^2P$ and $[1s2p^{5\,1}P]\epsilon p\,^2S - [2p^{4\,1}D]\epsilon p\,^2P$ transitions to be concerned with. On the basis of energy considerations, these transitions can be identified as α_3 and α_4, respectively. Since the intensity is proportional to the production probability times the emission probability, the diagonalization of the matrix (8) and the calculation of the line strengths yields the intensity ratio $r = I(\alpha_3)/I(\alpha_4)$. Furthermore, since the monopole selection rules prevent shake excitations to the triplet states $| \, t \, \rangle$, the result is

$$r = \frac{3}{5}(C_{1s}/C_{2s})^2$$
$$= (12\delta^2/5)\{E_s - E_t + [(E_s - E_t)^2 + 4\delta^2]^{1/2}\}^{-2}, \quad (9)$$

where the nondiagonal element $\delta = (\sqrt{3}/2)(G_c^1 - G^1)$ must eventually be interpreted as an effective exchange interaction if several ϵp spectator states are involved. In the weak-coupling limit, $G^1 \simeq G^0 \simeq 0$ in the matrix (8). Consequently, the ratio (9) is equal to the statistical ratio 9:5. From this maximum value, r decreases rapidly as the exchange interaction between ϵp and the core increases. This can be seen by studying r as a function of the reduced energy variable $\delta/(E_s - E_t)$. According to Eq. (9), $r = \frac{3}{5}$ for $E_t = E_s$, i.e., $G^0 = \frac{1}{18}(G_c^1 + G^1)$. It becomes less than $\frac{1}{20}$ in the strong-coupling limit $G^0 \simeq G_c^1$. The decrease of r is accompanied by a shift of both α_3 and α_4 which is rather difficult to predict.

Since r is extremely sensitive to the exchange interaction between the excited shake electron and the $1s2p^5$ core, the crystal environment of O^{2-} may have a dramatic effect on it.[30] Consider the rocksalt-type crystals MgO and CaO. According to Sec. VII A the creation of the O^{2-} $1s$ hole in CaO leads to the formation of localized $2p_{\nu}$ $(\nu = x,y,z)$ states in both the O^{2-}-Ca^{2+} z direction and the O^{2-}-O^{2-} x and y directions. In MgO this only occurs in the z direction since the excitation is shared by the neighboring oxygen ions in the x and y directions. Nevertheless, in both crystals there may be a distinct difference between the distribution of ϵp_z and $\epsilon p_{x,y}$ states. In the z direction the shake electron may be trapped in a discrete state of the positive ion, whereas no such states are available in the x and y directions.

The following argument indicates that the excitation of the $2p_z$ electron into an ϵp_z state may be very selective,

and that the electron may actually remain bound to the $1s\,2p^5$ oxygen core rather than go over to the positive ion. The reason is that the shake electron may become trapped by a positive potential barrier since the attractive positive-ion potential energy $-V(R)$ is superimposed in accordance with Eq. (6) on the slowly varying repulsive Madelung and polarization energies $V_M(R)+V_P(R)$. In order to get an estimate of this delicate situation, we have calculated the effective HF potential for the Mg^+ $3s$ and Ca^+ $4s$ states, respectively, and compared the results with Mahan's[21] values for $V_M(0)=E_M(1)$ and $V_P(0)=E_P(1)$. The HF potentials simulate $-V(R)$ for the lowest bound states into which the shake electron can go. It was found that, for both MgO and CaO,

$$\Delta = V_M(d/2)+V_P(d/2)-V(d/2)$$

$$\simeq V_M(0)+V_P(0)-V(d/2)\simeq +3 \text{ eV} ,$$

where d is the distance between O^{2-} and the positive ion. This result suggests that the shake electron may become trapped by a barrier in a very localized excitonlike state, in analogy with uv and x-ray absorption[31] of ionic crystals.

The arguments leading to Eq. (9) remain valid for a cubic crystal environment. Hence one may estimate the ratio (9) in MgO and CaO by assuming as anticipated above that the sudden change of $2p_z$ into $2p_z^*$ results predominantly in the formation of one very bound state. Since this change is the only excitation mechanism which contributes to the separate satellite emission in MgO, the strong-coupling limit prevails with the result that $I(\alpha_3)\simeq 0$ and $I\simeq I(\alpha_4)$ in agreement with Fig. 1. In CaO the sudden change of $2p_{x,y}$ into $2p_{x,y}^*$ is expected to correspond to the weak-coupling limit, in contrast to the change from $2p_z$ into $2p_z^*$. Hence, according to Eq. (9), r does not attain its maximum value of $\frac{9}{5}$, but is instead given by $r\simeq (\frac{2}{3})(\frac{9}{5})=\frac{6}{5}$, in good agreement with the experimental results for CaO, SrO, and BaO, as shown in Fig. 1 for SrO. According to Fig. 1, $0<r<1$ for Li_2O. This agrees with the conclusions of Sec. VI A that the separate satellite structure is due to the localization of $2p_{x,y}$ with x and y pointing toward the Li^+ ions. The angular distribution of the corresponding shake electrons is given by x^2+y^2, which is symmetric in the plane of the Li^+ ions. Hence only a fraction of the electrons is emitted toward the Li^+ ions, for which r would be zero if there would be a barrier.

VII. DISCUSSION

According to Sec. III and Fig. 1 there is a broad additional satellite structure above $+4$ eV in every oxide K-emission spectrum recorded so far. On the basis of our modified HF calculations, we attribute this peak to a superposition of $1s^{-1}2p^{-2}\text{-}2p^{-3}$ multiplets.[32] Since it appears with approximately the same intensity ($\simeq 7\%$) in all targets, the initial $1s^{-1}2p^{-2}$ triple-hole states seem to be completely localized and nonbonding regardless of the

crystal environment. This conclusion is in accordance with observations concerning the $K\text{-}VV$ Auger-electron spectra in various oxides including MgO.[33] In the MgO spectrum the strongest peak can be identified as consisting of the $1s^{-1}\text{-}2p^{-2}\,^1D$ and ^1S multiplets, just as in the neon $K\text{-}LL$ Auger spectrum. Hence the hole-hole correlation[5] is so strong in the valence band of MgO that the V^{-2} states become localized and nonbonding $2p^{-2}$ states even in the absence of the $1s$ hole. This result also rules out any final-state effects as being the reason for the difference between the (a)- and (b)-type $1s^{-1}V^{-1}\text{-}V^{-2}$ satellite structures.

In analogy to models[6,34] which have been used to explain the dependence of the F^- $1s^{-1}2p^{-1}\text{-}2p^{-2}$ satellite intensity on bonding in fluorides, one may also consider the possibility that a fraction of O^{2-} $1s^{-1}2p^{-1}$ states decays into O^{2-} $1s^{-1}$ and positive-ion $2p^{-1}$ states before the $1s$ hole is filled. This would lead to a smaller satellite intensity than predicted by the ion model in Sec. V B. We have checked this hypothesis for MgO by a calculation of the corresponding ionization energies. Using Mahan's results[21] in Eq. (6), the O^{2-} $1s^{-1}2p^{-1}$ double-ionization energy was found to be 550 eV, which is about 30 eV less than the sum of the Mg^{2+} $2p^{-1}$ and O^{2-} $1s^{-1}$ ionization energies. Hence the electron transfer from O^{2-} $1s^{-1}2p^{-1}$ to O^{2-} $1s^{-1}$ Mg^{2+} $2p^{-1}$ is energetically forbidden.

Our interpretation of the oxygen K-emission spectrum is relevant for the understanding of bonding effects in other anion x-ray emission spectra as well. Here we would only like to refer to the puzzling question regarding the very narrow Cl^- $K\beta_1$ line in KCl.[1] As far as we know no frozen-core calculation based on Eq. (1) has ever been able to reproduce the observed half-maximum width of 0.6 eV,[1] corrected for the $1s$ lifetime. The shape of the line is also at variance with band calculations.[11] Since $K\beta_1$ is accompanied by an intense satellite structure which can be interpreted in terms of $1s^{-1}3p^{-1}\text{-}3p^{-2}$ transitions, this could be an initial-state relaxation effect. Assuming a free Cl ion the shake theory predicts an intensity value which is in good agreement with experiments.[17] However, the satellite intensity becomes dramatically smaller in more covalent crystals.[35] Hence the situation is analogous to the change from (a)- to (c)-type oxygen spectra.

In conclusion, it has been shown that a direction-dependent initial-state relaxation mechanism accounts for the gradual disappearance of the oxygen $1s^{-1}V^{-1}\text{-}V^{-2}$ satellite structure in conjunction with the change from an almost free-ion-like to a bond-like $1s^{-1}\text{-}V^{-1}$ emission. Numerous consequences for other oxygen and anion core spectra remain to be explored.

ACKNOWLEDGMENTS

[1]L. G. Parratt, Rev. Mod. Phys. 31, 616 (1959).

[2]C.-O. Almbladh and L. Hedin, in *Handbook on Synchrotron Radiation,* edited by E. E. Koch (North-Holland, Amsterdam, 1983), Vol. 1, p. 607, and references therein.

[3]A. Meisel, G. Leonhardt, and R. Szargan, *Röntgenspektren und Chemische Bindung* (Geest-Portig, Leipzig, 1977), Chap. 7; C. Senemaud, in *Advances in X-Ray Spectroscopy,* edited by C. Bonnelle and C. Mande (Pergamon, Oxford, 1982), p. 423.

[4]G. A. Rooke, in *X-Ray Spectroscopy,* edited by L. V. Azaroff (McGraw-Hill, New York, 1974), p. 173.

[5]D. R. Jennison, J. A. Kelber, and R. R. Rye, Phys. Rev. B 25, 1384 (1982).

[6]O. Benka, R. L. Watson, and R. A. Kenefick, Phys. Rev. Lett. 47, 1202 (1981).

[7]H.-U. Chun and D. Hendel, Z. Naturforsch. 22a, 1401 (1967).

[8]S. P. Kowalczyk *et al.,* Solid State Commun. 23, 161 (1977).

[9]B. Fischer, R. A. Pollak, T. H. DiStefano, and W. D. Grobman, Phys. Rev. B 15, 3193 (1977).

[10]H. Van Doveren and J. A. Th. Verhoeven, J. Electron Spectrosc. Relat. Phenom. 21, 265 (1980).

[11]S. T. Pantelides, Phys. Rev. B 11, 5802 (1975).

[12]N. Daude, C. Jouanin, and C. Gout, Phys. Rev. B 15, 2399 (1977).

[13]I. P. Batra, J. Phys. C 15, 5399 (1982).

[14]K. J. Chang, S. Froyen, and M. L. Cohen, J. Phys. C 16, 3475 (1983).

[15]J. R. Chelikowsky and M. Schlüter, Phys. Rev. B 15, 4020 (1977); see also S. T. Pantelides and W. A. Harrison, *ibid.* 13, 2667 (1976).

[16]The (a)- and (b)-type materials in Table I have a rocksalt structure, except for Li_2O, which has an antifluorite structure. BeO and SiO_2 are hexagonal, whereas Al_2O_3 is rhombohedral.

[17]R. Åberg, Phys. Rev. 156, 35 (1967); T. Åberg, in *Proceedings of the International Conference on Inner-Shell Ionization Phenomena and Future Applications,* edited by R. W. Fink, S. T. Manson, J. M. Palms, and P. Venugopala Rao, U.S. Atomic Energy Commission Report No. CONF-720404 (National Technical Information Service, U.S. Dept. of Commerce, Springfield, Va., 1972), p. 1509.

[18]P. S. Bagus and C. W. Bauschlicher, Jr., J. Electron Spectrosc. Relat. Phenom. 20, 183 (1980).

[19]R. E. Watson, Phys. Rev. 111, 1108 (1958).

[20]G. D. Mahan, Phys. Rev. B 21, 4791 (1980).

[21]G. D. Mahan, Phys. Rev. B 22, 3102 (1980).

[22]I. A. Brytov and Yu. N. Romashchenko, Fiz. Tverd. Tela (Leningrad) 20, 664 (1978) [Sov. Phys.—Solid State 20, 384 (1978)].

[23]O. Keski-Rahkonen, Phys. Scr. 7, 173 (1973).

[24]T. Åberg, K. Reinikainen, and O. Keski-Rahkonen, Phys. Rev. A 23, 153 (1981).

[25]W. A. Harrison, *Electronic Structure and the Properties of Solids* (Freeman, San Francisco, 1980), p. 264.

[26]I. M. Antova, Phys. Status Solidi B 94, K165 (1979).

[27]R. Manne and T. Åberg, Chem. Phys. Lett. 7, 282 (1970).

[28]M. O. Krause, T. A. Carlson, and R. D. Dismukes, Phys. Rev. 170, 37 (1968).

[29]D. Chattarji, W. Mehlhorn, and V. Schmidt, J. Electron Spectrosc. Relat. Phenom. 13, 97 (1978).

[30]According to our Hartree-Fock (HF) calculations, $r \simeq 1$ for initial $1s\,2p^5 3p$ free-oxygen-pseudoion states.

[31]T. Åberg and J. L. Dehmer, J. Phys. C 6, 1450 (1973); S. T. Pantelides, Phys. Rev. B 11, 2391 (1975).

[32]According to our HF results, $E_{av}(1s^{-1}2p^{-2}) - E_{av}(2p^{-3}) - E(K\alpha) = +4.7$ eV (av represents average), in good agreement with the position of the second satellite structure.

[33]J. C. Fuggle, E. Umbach, R. Kakoschke, and D. Menzel, J. Electron Spectrosc. Relat. Phenom. 26, 111 (1982).

[34]M. Uda *et al.,* Phys. Rev. Lett. 42, 1257 (1979).

[35]S. Muramatsu and C. Sugiura, Phys. Rev. B 27, 3806 (1983).